Original Article

MPP7 is a potential prognostic marker and is associated with cancer metabolism and immune infiltration in clear cell renal cell carcinoma: a bioinformatics analysis based on the TCGA database

Xiaowei Cheng[1#], Ding Sun[1#], Hao Li[1], Jie Zhang[1], Qing Luo[1], Xinye Jin[1], Yizhi Chen[1,2], Qing Yuan[3], Bin Wang[1,2]

[1]Department of Nephrology, Hainan Hospital of Chinese PLA General Hospital, the Hainan Academician Team Innovation Center, Sanya, China; [2]Senior Department of Nephrology, the First Medical Center of Chinese PLA General Hospital, Chinese PLA Institute of Nephrology, State Key Laboratory of Kidney Diseases, National Clinical Research Center for Kidney Diseases, Beijing Key Laboratory of Kidney Diseases Research, Beijing, China; [3]Senior Department of Urology, the Third Medical Center of Chinese PLA General Hospital, Beijing, China

Contributions: (I) Conception and design: B Wang, Q Yuan, X Cheng, D Sun; (II) Administrative support: Q Yuan, B Wang; (III) Provision of study materials or patients: Y Chen; (IV) Collection and assembly of data: X Cheng, D Sun; (V) Data analysis and interpretation: X Cheng, D Sun, H Li, J Zhang, Q Luo, X Jin, Y Chen; (VI) Manuscript writing: All authors; (VII) Final approval of manuscript: All authors.

[#]These authors contributed equally to this work.

Correspondence to: Dr. Bin Wang. Department of Nephrology, Hainan Hospital of Chinese PLA General Hospital, the Hainan Academician Team Innovation Center, No. 80 of Jianglin Road, Haitang District, Sanya 572013, China. Email: binwang2000@aliyun.com; Dr. Qing Yuan. Senior Department of Urology, the Third Medical Center of Chinese PLA General Hospital, No. 69 of Yongding Road, Haidian District, Beijing 100853, China. Email: qyuanmd@outlook.com.

Background: Metastasis is a major negative prognostic marker in clear cell renal cell carcinoma (ccRCC). Membrane palmitoylated proteins (MPPs) are a class of cell polarity-associated proteins that function in both cell-cell junction and adhesion. However, the relationship between *MPP7* and the prognosis of ccRCC remains elusive. In this study, we aimed to investigate the associations between *MPP7* expression with clinical prognosis of ccRCC using bioinformatics analyses.

Methods: The messenger RNA (mRNA) and protein expression patterns of *MPP7* in different cancer types were examined using The Cancer Genome Atlas (TCGA) and Human Protein Atlas (HPA) databases, with key clinical characteristics (TNM and pathological stages, pathological grade, survival status) included. A nomogram model using *MPP7* expressions and other clinical factors was built to predict the survival probability. The Kaplan-Meier plotter and Cox regression were employed to investigate the clinical significance and prognostic value of *MPP7* in ccRCC. *MPP7* expression-associated signaling pathways with were analyzed by the Gene Ontology (GO) and Kyoto Encyclopedia of Genes and Genome (KEGG) tools. The Tumor Immune Estimation Resource (TIMER) database was used to investigate the correlation between *MPP7* and the infiltration patterns of immune cells.

Results: By analyzing TCGA-kidney renal clear cell carcinoma (TCGA-KIRC) and HPA databases, we found that *MPP7* was differentially expressed in tumor tissues and adjacent normal tissues (P<0.001). The *MPP7* expression patterns were associated with pathological stage (P<0.001), histological grade (P<0.01), and survival status (P<0.001). Using nomogram model, Cox regression and survival analysis, it showed that *MPP7* expressions combined with key clinical factors could accurately predict the clinical prognosis. The promoter methylation patterns of *MPP7* were correlated with the clinical factors of ccRCC patients. Furthermore, the KEGG and GO analyses demonstrated that *MPP7* is associated with mitochondrial oxidative metabolism. *MPP7* expression was associated with multiple types of immune cells and correlated with the enrichment of these cells.

Conclusions: *MPP7* is a critical gene links with ccRCC prognosis and is associated with tumor immune status and metabolism. *MPP7* could become a potential biomarker and important therapeutic target for ccRCC patients.

Keywords: Clear cell renal cell carcinoma (ccRCC); membrane palmitoylated protein-7 (MPP7); infiltrating immune cells; invasion; mitochondrial metabolism

Submitted Feb 27, 2023. Accepted for publication Apr 21, 2023. Published online Apr 28, 2023.
doi: 10.21037/tau-23-166
View this article at: https://dx.doi.org/10.21037/tau-23-166

Introduction

According to the latest statistics, renal cancer is the most common type of tumor in the urinary system, with an increasing incidence in both genders in the United States (1). Clear cell renal cell carcinoma (ccRCC) is an aggressive subtype of renal cancer, accounting for 90% of cases and the majority of deaths of renal cancer. Owing to the lack of typical clinical symptoms, approximately 25–30% of patients with ccRCC have already developed distant metastases upon diagnosis (2,3). In addition, improvement via surgical nephrectomy achieves a good prognosis for early-stage ccRCC patients; however, the 5-year survival rate of patients with advanced ccRCC is still less than 10% (4). Novel therapeutics such as antiangiogenic therapy, immune checkpoint inhibitors, tyrosine kinase inhibitors, and mammalian target of rapamycin (mTOR) inhibitors have brought hope to advanced ccRCC patients. Yet, the prognoses of metastatic ccRCC patients are still poor (5). Therefore, investigating the metastatic mechanisms of ccRCC is important for determining its pathogenesis and developing therapeutic options for ccRCC patients.

A previous study indicated that cell polarity is important for tumor pathogenesis and progression. Changes in the polarity-associated protein expression patterns have been shown to affect epithelial polarity, thereby regulating cell proliferation, migration, and tumorigenesis (6). The membrane-associated guanylate kinases (MAGUKs) are a class of scaffolding-associated proteins, which play key roles in cell adhesion, cell junctions, and cell polarity (7). Moreover, MAGUKs can be divided into several subfamilies according to their structural features, including the membrane palmitoylated protein (MPP) subfamily (8). It was reported that MPPs are a class of cell polarity-associated proteins, which function effectively in both cell junctions and adhesion (8). Recent studies have indicated that MPPs also function in tumorigenesis. For instance, *MPP2* was reported to regulate the activity of the oncogene s-Src (9). Moreover, the downregulation of *MPP6* is associated with ovarian cancer progression (10). Furthermore, *MPP6* suppression ameliorates the anti-cancer activity of Saa3-knockout cancer-associated fibroblasts (11). *MPP7* was also shown to function in both pancreatic ductal adenocarcinoma and breast cancer via the modulation of autophagy and activation of the epidermal growth factor receptor (EGFR)/protein kinase B (AKT) signaling, respectively (12,13). However, whether *MPP7* functions in the pathogenesis and progression of ccRCC with the possible mechanisms are still not clear. Previous studies indicate that several biomarkers correlate with the clinical prognoses of ccRCC patients. For instance, PTP4A3, GPX1, TAZ were all reported with the clinical prognosis of renal cancer and function via different signaling pathways (14-16). However, the association between MPPs and ccRCC has not been reported before. Therefore, we intended to investigate the potential role of *MPP7* in ccRCC by conducting bioinformatics-based analyses using a variety of databases and tools.

In this multi-dimensional bioinformatics-based study, we tried to analyze the associations between *MPP7* and the clinical prognosis, while investigating the corresponding

Highlight box

Key findings

- Using multi-dimensional bioinformatics analyses, we found that *MPP7* is a critical gene whose expression level is significantly correlated with ccRCC prognosis, regulating tumor immune status and metabolism.

What is known and what is new?

- Metastasis is a major negative prognostic marker in ccRCC. MPPs are a class of cell polarity-associated proteins, which function in both cell junctions and adhesion.
- *MPP7* is differentially expressed in tumor and paracancerous tissues and is correlated with the clinical prognosis. Moreover, *MPP7* also correlates with mitochondrial metabolism and immune cell infiltration.

What is the implication, and what should change now?

- *MPP7* could become a potential prognostic and therapeutic target for ccRCC, combined with other key factors. However, more *in vivo* experiments are still needed to validate the role of *MPP7* in cancer.

relations by data analyses. Data from The Cancer Genome Atlas-kidney renal clear cell carcinoma (TCGA-KIRC) were used to investigate the associations between the *MPP7* expression and clinical prognoses [tumor-node-metastasis (TNM) stages, pathological grades, survival status, etc.] in ccRCC patients. Also, the MPP7 levels combined with other clinical factors were used to predict the clinical prognoses of ccRCC patients. Meanwhile, Kyoto Encyclopedia of Genes and Genome (KEGG) and Gene Ontology (GO) analyses were performed and the promoter methylation status of *MPP7* was further analyzed. In addition, the correlations between *MPP7* expressions and immune infiltration status were also investigated. Our study reveals the significance of *MPP7* in ccRCC and its fundamental role in cancer metabolism, immunity, and tumorigenesis. We present the following article in accordance with the REMARK reporting checklist (available at https://tau.amegroups.com/article/view/10.21037/tau-23-166/rc).

Methods

Gene expression profile analysis

This retrospective study analyzed the *MPP7* levels and clinical prognoses of ccRCC patients. The messenger RNA (mRNA) expressions of *MPP7* were analyzed by investigating the Tumor Immune Estimation Resource (TIMER) database according to the clinical data uploaded from TCGA (17). The TCGA-KIRC cohort consisted of 539 patients with ccRCC, including 539 tumor samples with 72 adjacent normal tissues, combined with the clinical prognoses and key information. Moreover, two Gene Expression Omnibus (GEO) datasets were analyzed to investigate the *MPP7* expression patterns in the normal and tumor tissues. To further validate the expression profiles of *MPP7*, the Human Protein Atlas (HPA) database (18) was utilized to confirm the expression levels in ccRCC and adjacent tissues by immunohistochemical (IHC) staining. The study was conducted in accordance with the Declaration of Helsinki (as revised in 2013).

Correlation analysis of MPP7 expression and clinical prognosis

The associations between *MPP7* mRNA levels and the key clinicopathological characteristics, including T and N stages, M status, pathological stages, histological grades, gender, age, and survival status [overall survival (OS), disease-specific survival (DSS), and progression-free interval (PFI)], were determined using data from TCGA-KIRC cohort and the ggplot2 R package (R Foundation for Statistical Computing, Vienna, Austria).

Overall and disease-associated survival analyses

The Kaplan-Meier online database (https://kmplot.com/analysis/) was used to assess the associations between *MPP7* and the cumulative survival rates of cancer patients based on data from TCGA-KIRC cohort. Specifically, the OS, DSS, and PFI were determined by classifying the ccRCC patients into two groups by the median *MPP7* expression value. Log-rank tests with P values and hazard ratios (HRs) with 95% confidence intervals (CIs) were also analyzed. The time-dependent receiver operator characteristic (ROC) curves and a nomogram model graph were plotted using the timeROC, "Survival", "survminer", and "rms" R packages for prognosis prediction, based on data from TCGA-KIRC cohort. Moreover, prognosis-associated calibration analyses were conducted by incorporating the key prognosis-associated factors with the predicted 1-, 3-, and 5-year survival rates using the 'rms' R package.

Methylation analysis of MPP7 in ccRCC

A comprehensive analysis of the relationship between *MPP7* methylation and clinical characteristics, including cancer type and stage, histological grade, gender, and age, was conducted using the University of Alabama Cancer Database (UALCAN) website. In addition, the significance of different methylation sites from TCGA cohort was explored using the online MethSurv tool (19). To determine the mechanisms of *MPP7* dysregulations, mutation levels were also presented using the cBioPortal tool for cancer genomics based on TCGA PanCancer Atlas Studies.

Single-cell analysis of MPP7 in the functional states of ccRCC

The CancerSEA website (http://biocc.hrbmu.edu.cn/CancerSEA) was used to analyze the roles of specific genes in the cancer hallmarks of certain cancer types. These phenotypes include angiogenesis, cell apoptosis, cell cycle progression, cell differentiation, DNA damage/repair, epithelial-mesenchymal transition, hypoxia, inflammation status, cell invasion, metastatic status, cell proliferation, cell quiescence, and stemness properties. The results were based

on certain single-cell sequencing study to provide more clinical information.

GO and KEGG analyses

To determine the associations between *MPP7* and ccRCC, both the co-expressed genes and the differentially expressed genes (DEGs) were screened using the "limma" and "DESeq2" packages in R software (20). GO and KEGG analyses were performed using the "clusterProfiler" R package to explore biological functions and signal channels associated with *MPP7*. The GO analyses mainly included biological process (BP), cell composition (CC), and molecular function (MF) analyses (21). The STRING tool was used to investigate the functional association network of *MPP7* with other proteins (22).

Correlations between MPP7 and immune-infiltrating cells

The TIMER database was adopted to further investigate the associations between the infiltration patterns of immune cells and *MPP7* expressions (23). The CIBERSORT tool (24) was adopted to quantify the percentages of immune cells in ccRCC samples by classifying these participants according to their *MPP7* expression levels. The "ggplot2", "tidyverse", and "reshape2" R packages were adopted. Meanwhile, the TIMER website and the Kaplan-Meier curves were used to investigate and visualize the correlations between infiltrating immune cells and the clinical prognoses of these patients.

Statistical analysis

SPSS software (version 20.0, SPSS Inc., Chicago, IL, USA) and R software (version 4.0.4, R Foundation for Statistical Computing, Vienna, Austria) were utilized for all statistical analyses in this study. The clinical data in this study are presented as the mean ± standard deviation (SD). Specifically, Student's *t*-tests of both independent and paired samples were performed to analyze the *MPP7* expression difference among different groups. The chi-squared test was used to analyze the *MPP7* proportion difference in different groups in terms of the key clinical characteristic variables. The Cox proportional hazards regression models were constructed in both univariate and multivariate manners, adjusting for confounding factors. The OS, DSS, and PFI analyses were conducted using the Kaplan-Meier plots and log-rank tests. A two-tailed P<0.05 was considered to indicate a statistically significant difference.

Results

MPP7 expression is decreased in ccRCC compared with normal tissue

By analyzing the Pan-Cancer TCGA data, we found that *MPP7* exhibited decreased expression patterns in several key cancer types (*Figure 1A*). Therefore, we mainly concentrated on the role of *MPP7* in renal cancers, especially the ccRCC. More specifically, KIRC tissues exhibited decreased *MPP7* expression using both the unpaired and paired data (P<0.001; *Figure 1B*). Furthermore, the expression patterns of *MPP7* were further validated using the GEO datasets, GSE100666 (n=3 in each group) and GSE66270 (n=14 in each group), which revealed that *MPP7* expression was lower in tumor tissues compared to the normal controls (*Figure 1C,1D*). The HPA database analysis showed via IHC staining that the *MPP7* protein was weakly expressed in tumor tissues compared with adjacent normal tissues (*Figure 1E*).

MPP7 expression is correlated with the clinical prognosis of ccRCC patients

The included ccRCC patients were further classified into high (n=270) and low (n=269) *MPP7* groups in TCGA-KIRC cohort. Their baseline characteristics are presented in *Table 1*, which showed that *MPP7* expression levels were correlated with T stages, M stages, pathologic stages, and histologic grades (P<0.001). Moreover, *MPP7* expression was downregulated and the number of T stages was increased, with significant differences detected between patients with T1 and T4 stages (P<0.001; *Figure 2A*). Meanwhile, patients with N1 and N0 stages exhibited no difference of *MPP7* expressions, while those with M1 stage had lower *MPP7* expression levels than those with M0 stage (P<0.001; *Figure 2B,2C*).

Moreover, ccRCC patients with a higher pathologic stage or histologic grade exhibited decreased *MPP7* levels than those with a lower stage or grade (*Figure 2D,2E*). There were no significant differences in *MPP7* levels between females and males or between elderly (>60 years) and younger (≤60 years) patients (*Figure 2F,2G*). Furthermore, according to the survival outcomes, dead patients exhibited reduced *MPP7* levels compared to those in live patients (*Figure 2H-2J*).

Univariate Cox analysis revealed that except for

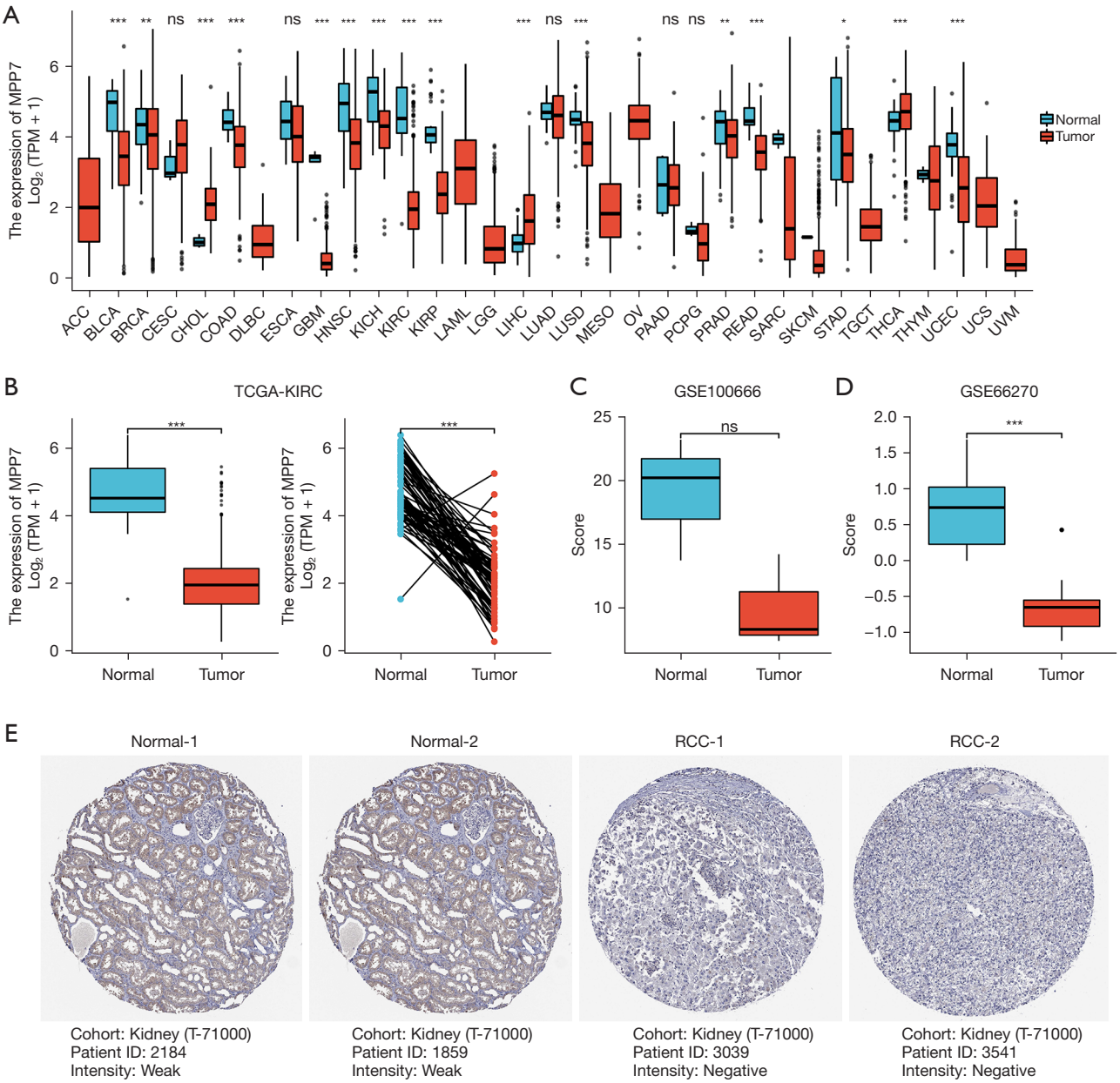

Figure 1 Dysregulated *MPP7* expression profiles between tumor and adjacent tissues of ccRCC. (A) The *MPP7* expression levels in 26 types of cancer and normal tissues (TCGA cancer data vs. TCGA normal data). (B) The *MPP7* expression levels in unpaired (n=72 in normal group and n=539 in tumor group) and paired (n=72) patients from the TCGA-KIRC cohort. (C,D) The *MPP7* expression patterns of samples from the GSE100666 (n=3 in each group) and GSE66270 (n=14 in each group) datasets. (E) IHC staining (50×) was used to confirm the expression levels in ccRCC and adjacent tissues from the HPA database, with the cohort and patients' ID listed. URL of each panel: normal-1 (patient ID: 2184) and normal-2 (patient ID: 1859): https://www.proteinatlas.org/ENSG00000150054-MPP7/tissue/kidney#img. RCC-1 (patient ID: 3039) and RCC-2 (patient ID: 3541): https://www.proteinatlas.org/ENSG00000150054-MPP7/pathology/renal+cancer#img. *P<0.05; **P<0.01; ***P<0.001; ns, P>0.05. *MPP7*, membrane palmitoylated protein-7; TPM, transcripts per million; TCGA, The Cancer Genome Atlas; KIRC, kidney renal clear cell carcinoma; RCC, renal cell carcinoma; ccRCC, clear cell renal cell carcinoma; IHC, immunohistochemical.

Table 1 The baseline characteristics of patients with ccRCC according to the expression levels of *MPP7* in TCGA-KIRC cohort

Characteristics	Low *MPP7*	High *MPP7*	P value
Sample size	269	270	–
T stage, n (%)			<0.001
T1	118 (43.9)	160 (59.3)	
T2	33 (12.3)	38 (14.1)	
T3	110 (40.9)	69 (25.6)	
T4	8 (3.0)	3 (1.1)	
N stage, n (%)			0.160
N0	114 (42.4)	127 (47.0)	
N1	11 (4.1)	5 (1.9)	
M stage, n (%)			<0.001
M0	196 (72.9)	232 (85.9)	
M1	56 (20.8)	22 (8.1)	
Pathologic stage, n (%)			<0.001
Stage I	114 (42.4)	158 (58.5)	
Stage II	25 (9.3)	34 (12.6)	
Stage III	70 (26.0)	53 (19.6)	
Stage IV	59 (21.9)	23 (8.5)	
Histologic grade, n (%)			<0.001
G1	7 (2.6)	7 (2.6)	
G2	101 (37.5)	134 (49.6)	
G3	104 (38.7)	103 (38.1)	
G4	55 (20.4)	20 (7.4)	
Gender, n (%)			0.547
Female	89 (33.1)	97 (35.9)	
Male	180 (66.9)	173 (64.1)	
Age (years), n (%)			0.636
≤60	131 (48.7)	138 (51.1)	
>60	138 (51.3)	132 (48.9)	

ccRCC, clear cell renal cell carcinoma; MPP7, membrane palmitoylated protein-7; TCGA, The Cancer Genome Atlas; KIRC, kidney renal clear cell carcinoma.

gender, all of the key characteristics exhibited significant associations with the clinical prognosis, whereas only M stage, age, and *MPP7* expression levels were included in the final model during multivariate analysis (*Table 2*). These results suggested that *MPP7* expression patterns play vital roles in the clinical prognoses of ccRCC patients, combined with other key factors.

MPP7 is a prognostic factor that is associated with clinical outcomes in ccRCC patients

The prognostic value of *MPP7* in ccRCC was assessed by Kaplan-Meier analyses and log-rank tests. Low *MPP7* levels were associated with significantly decreased OS (HR =0.37, P<0.001; *Figure 3A*), DSS (HR =0.28, P<0.001; *Figure 3B*), and PFI (HR =0.43, P<0.001; *Figure 3C*), compared with higher *MPP7* expression in the TCGA-KIRC cohort.

For the time-dependent ROC curves, time-dependent survival ROC curves of *MPP7* were created to predict the 1-, 3-, and 5-year survival rates. However, all of these AUC values were lower than 0.6 (which was regarded as the threshold value, *Figure 3D*), indicating that *MPP7* alone is not a suitable index to predict the time-dependent prognosis.

By combining the key clinicopathological factors (age, sex, T stage, N stage, M stage, and histological and pathological stages) and *MPP7* expression, we built a nomogram model that can be used to predict the survival probabilities at 1-, 3-, and 5-year for patients in clinical practice (*Figure 3E*), indicating that the model combining *MPP7* expression with other clinical factors is a dominant factor in predicting survival probability for ccRCC patients. Moreover, prognosis-associated calibration analyses were conducted by incorporating *MPP7* expressions, M stages, and histologic grades, and demonstrated that these factors could perfectly predict the 1-, 3-, and 5-year survival probabilities (*Figure 3F-3H*).

Association of MPP7 methylation and mutation status with clinical features in patients with ccRCC

The associations between promoter methylation levels of *MPP7* and clinical features were analyzed, showing that ccRCC tumors exhibited increased methylation levels compared to those in normal tissues (P<1E-12; *Figure 4A*). Meanwhile, no significant differences were observed among different pathologic stages or histologic grades (*Figure 4B,4C*). A significant difference in methylation levels was observed between N0 and N1 (P<0.05; *Figure 4D*) but no significant differences were found between different age groups or genders (*Figure 4E,4F*).

Furthermore, the DNA methylation patterns of *MPP7* were assessed according to the prognostic value of

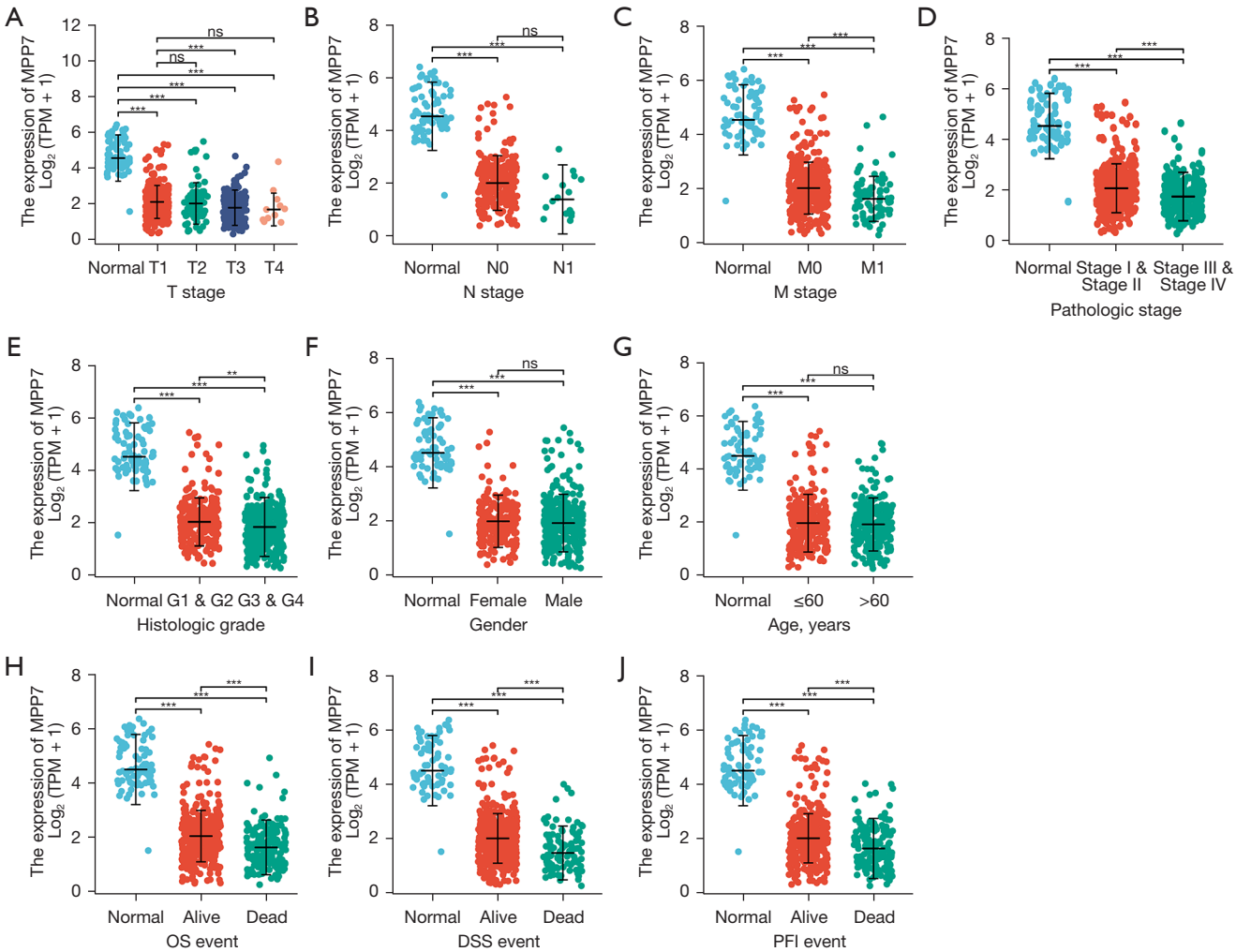

Figure 2 Relationship between the *MPP7* expression and clinicopathological parameters of ccRCC from the TCGA-KIRC cohort. Correlations between the expression patterns of *MPP7* and T stages (A), N stages (B), M status (C), pathological stages (D), histologic grades (E), gender (F), age (G), OS event (H), DSS event (I), and PFI event (J). **P<0.01; ***P<0.001; ns, P>0.05. *MPP7*, membrane palmitoylated protein-7; TPM, transcripts per million; OS, overall survival; DSS, disease-specific survival; PFI, progression-free interval; ccRCC, clear cell renal cell carcinoma; TCGA, The Cancer Genome Atlas; KIRC, kidney renal clear cell carcinoma.

each single cytosine-phospho-guanine (CpG) using the MethSurv tool. The MethSurv database results suggested 14 methylation CpG sites, among which most sites had a high level of DNA methylation (*Figure 4G*). The methylation levels of five CpG sites were correlated with prognosis: cg06308088, cg08505335, cg11601254, cg11952493, and cg17120366 (P<0.05; *Table 3*). Until now, no significant *MPP7* gene mutation data have been observed in ccRCC (*Figure 4H*).

Single-cell sequencing analysis revealed the role of MPP7 in ccRCC tissues

Based on data from the CancerSEA website, we found that no significant correlation existed between *MPP7* expression and the hallmarks of ccRCC (*Figure 5A*). A single-cell sequencing study on ccRCC (25) obtained a total of 83 cells, and the expression distribution was examined with a t-distributed stochastic neighbor embedding (t-SNE) plot

Table 2 Univariate and multivariate cox analyses of the key clinical characteristics in ccRCC

Characteristics	Total, n	Univariate analysis		Multivariate analysis	
		HR (95% CI)	P value	HR (95% CI)	P value
T stage	539				
T1 & T2	349	Reference			
T3 & T4	190	3.228 (2.382–4.374)	<0.001	1.453 (0.633–3.334)	0.378
N stage	257				
N0	241	Reference			
N1	16	3.453 (1.832–6.508)	<0.001	1.438 (0.715–2.894)	0.309
M stage	506				
M0	428	Reference			
M1	78	4.389 (3.212–5.999)	<0.001	2.299 (1.345–3.931)	0.002
Pathologic stage	536				
Stage I & II	331	Reference			
Stage III & IV	205	3.946 (2.872–5.423)	<0.001	1.348 (0.530–3.427)	0.531
Histologic grade	531				
G1 & G2	249	Reference			
G3 & G4	282	2.702 (1.918–3.807)	<0.001	1.586 (0.951–2.646)	0.077
Gender	539				
Male	353	Reference			
Female	186	1.075 (0.788–1.465)	0.648		
Age (years)	539				
≤60	269	Reference			
>60	270	1.765 (1.298–2.398)	<0.001	1.712 (1.114–2.631)	0.014
MPP7	539				
Low	269	Reference			
High	270	0.367 (0.266–0.505)	<0.001	0.423 (0.268–0.667)	<0.001

ccRCC, clear cell renal cell carcinoma; HR, hazard ratio; CI, confidence interval; MPP7, membrane palmitoylated protein-7.

(*Figure 5B,5C*). Moreover, *MPP7* expression was correlated with cell invasion in ccRCC, with a correlation of –0.39 and P<0.05 (*Figure 5D*).

GO and KEGG pathway analyses of MPP7

The top 100-most correlated genes with *MPP7* in the GO and KEGG enrichment analyses were determined using the "clusterProfiler" R package. Previous studies indicated that *MPP7* functions in the regulation of cell polarity and cell junctions. The GO analysis showed that most of the genes were associated with adenosine triphosphatase (ATPase) activity, proton transport, mitochondrial matrix, and the acetyl-CoA metabolic process (*Figure 6A*). The KEGG data suggested that oxidative phosphorylation and citrate cycle were related to the function of *MPP7* (*Figure 6B*). Moreover, *MPP7*-binding proteins were investigated using the STRING network (*Figure 6C*) and were combined with key genes on autophagy, metabolism, cell junction, etc.

To further investigate the signaling pathways associated with *MPP7*, DEGs exhibiting P<0.05 and $\log_2$fold change >2 were collected. Both GO and KEGG analyses

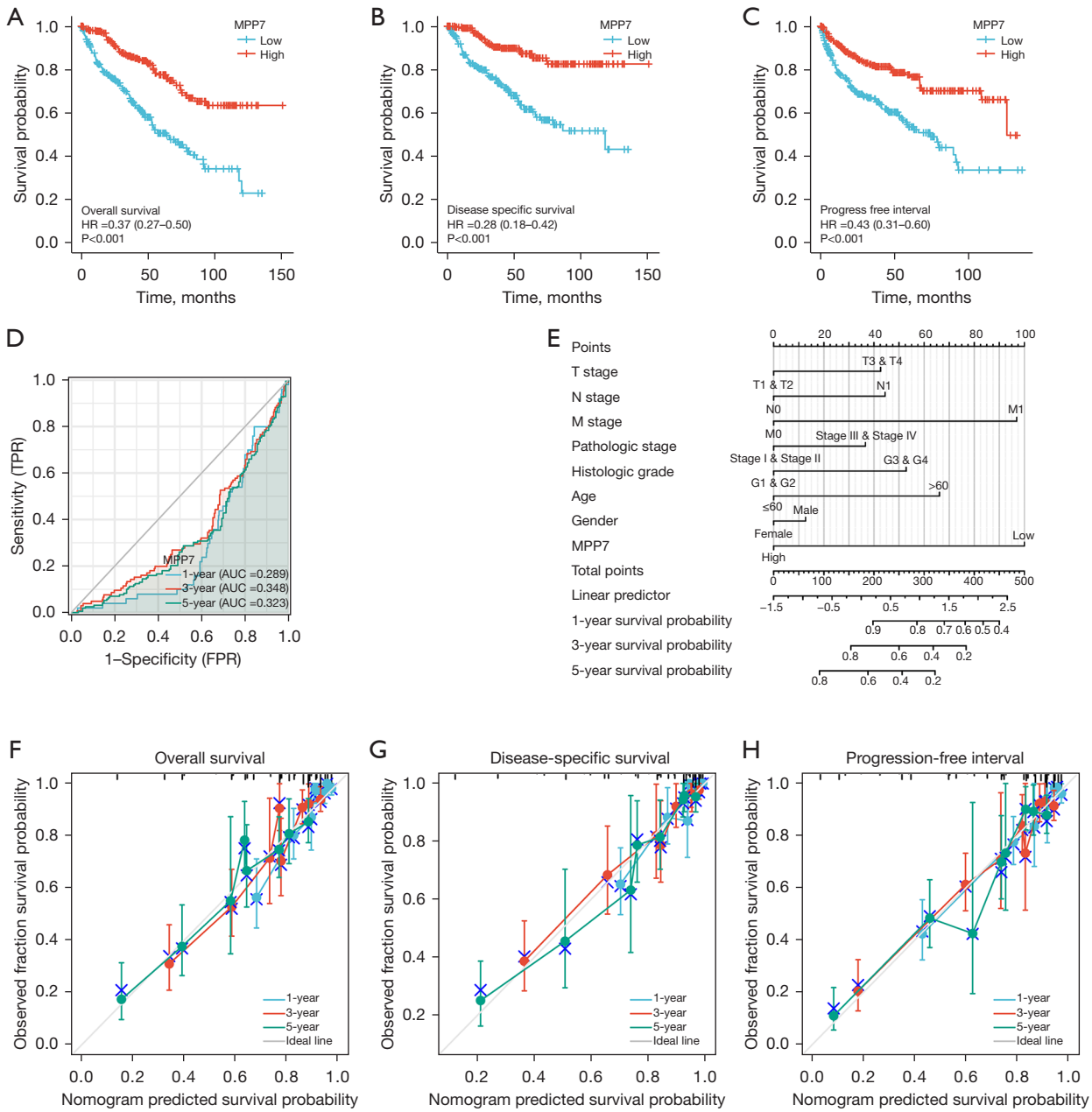

Figure 3 Prognostic and predictive value of *MPP7* expression in ccRCC patients from TCGA-KIRC cohort. (A-C) The OS, DSS, and PFI survival curves presenting patients with high (red) and low (blue) *MPP7* expression in ccRCC. (D) Time-dependent curve analysis to predict the 1-, 3-, and 5-year survival rates. (E) Nomogram model integrating the clinicopathologic factors and *MPP7* expression levels to predict the survival probability at 1, 3, and 5 years. (F-H) Prognosis-associated calibration analyses were conducted by incorporating the key prognosis-associated factors to predict the 1-, 3-, and 5-year OS, DSS, and PFI. *MPP7*, membrane palmitoylated protein-7; HR, hazard ratio; TPR, true positive rate; FPR, false positive rate; AUC, area under the curve; CI, confidence interval; ccRCC, clear cell renal cell carcinoma; TCGA, The Cancer Genome Atlas; KIRC, kidney renal clear cell carcinoma; OS, overall survival; DSS, disease-specific survival; PFI, progression-free interval.

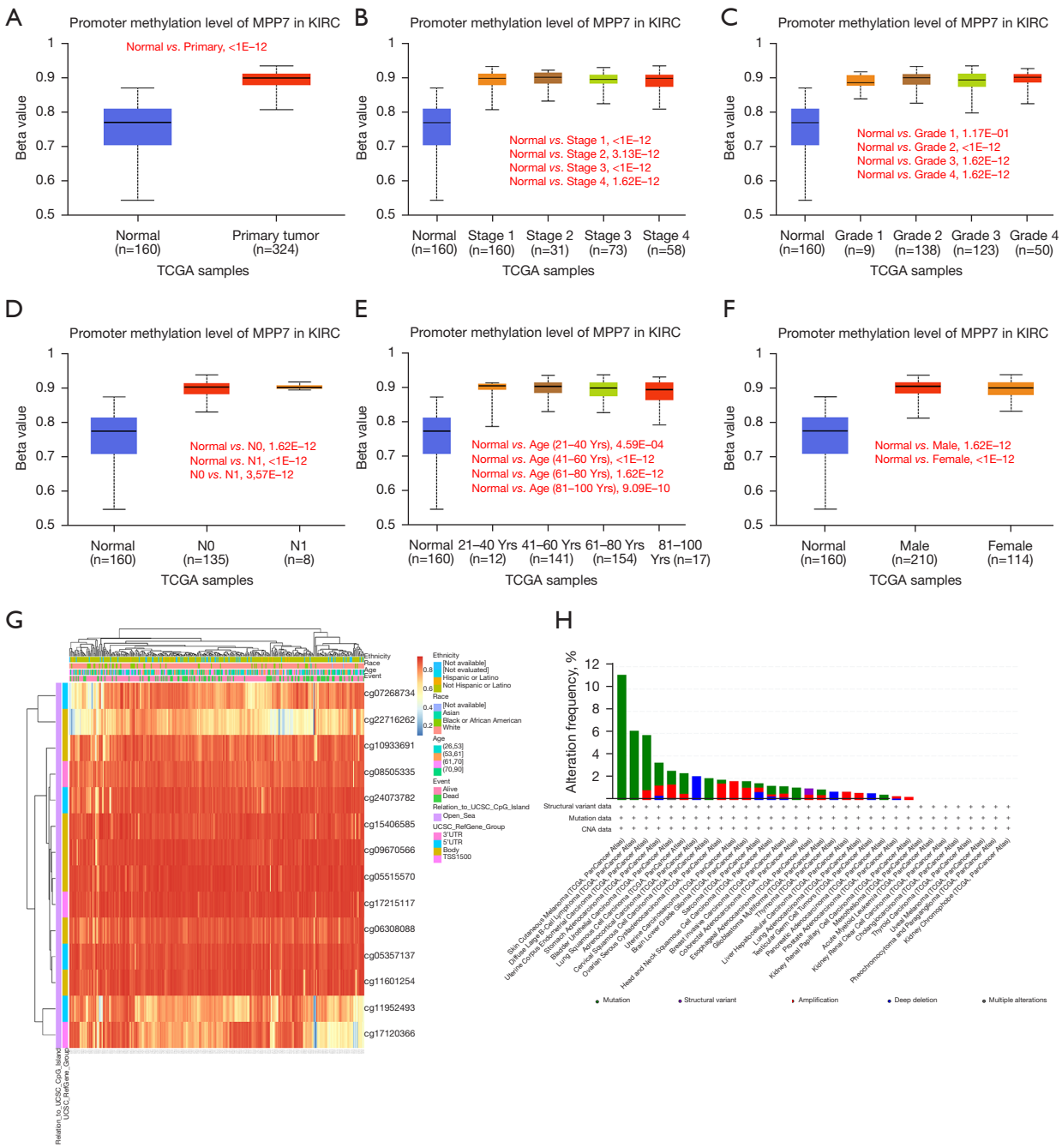

Figure 4 DNA methylation levels of *MPP7* with its prognostic value in ccRCC. (A) Promoter methylation patterns of *MPP7* in both normal and ccRCC tissues using the UALCAN database. (B-F) Promoter methylation level of *MPP7* in ccRCC cancer tissues of various tumor stages, tumor grades, nodal metastasis status, ages, and genders using the UALCAN database. (G) The heat map of DNA methylation at CpG sites in the *MPP7* gene by the MethSurv database. (H) The structural and mutation data of all cancer types from TCGA PanCancer data. *MPP7*, membrane palmitoylated protein-7; KIRC, kidney renal clear cell carcinoma; TCGA, The Cancer Genome Atlas; UCSC, University of California Santa Cruz; CNA, copy number alteration; ccRCC, clear cell renal cell carcinoma; UALCAN, University of Alabama Cancer Database; CpG, cytosine-phospho-guanine.

Table 3 The significant prognostic values of CpG in the MPP7 promoter

Gene symbol	CpG name	HR	95% CI	LR test P value	UCSC Ref gene group	Relation to UCSC CpG island
MPP7	cg05357137	0.652	0.424–1.003	0.059628	5'UTR	Open_Sea
	cg05515570	1.340	0.806–2.228	0.244227	Body	Open_Sea
	cg06308088	0.583	0.396–0.857	0.007021	Body	Open_Sea
	cg07268734	1.228	0.772–1.952	0.376782	5'UTR	Open_Sea
	cg08505335	1.737	1.033–2.923	0.027180	3'UTR	Open_Sea
	cg09670566	1.457	0.987–2.150	0.056424	Body	Open_Sea
	cg10933691	1.270	0.864–1.867	0.223664	Body	Open_Sea
	cg11601254	0.487	0.324–0.733	0.000981	Body	Open_Sea
	cg11952493	0.505	0.302–0.844	0.005223	5'UTR	Open_Sea
	cg15406585	0.640	0.398–1.028	0.054910	Body	Open_Sea
	cg17120366	0.400	0.265–0.604	5.86E-06	TSS1500	Open_Sea
	cg17215117	1.284	0.801–2.056	0.287787	TSS1500	Open_Sea
	cg22716262	0.705	0.469–1.058	0.098402	Body	Open_Sea
	cg24073782	1.295	0.847–1.980	0.242171	5'UTR	Open_Sea

CpG, cytosine-phospho-guanine; MPP7, membrane palmitoylated protein-7; HR, hazard ratio; CI, confidence interval; LR, likelihood ratio; UCSC, University of California Santa Cruz; UTR, untranslated region.

were performed using these DEGs, which showed that these DEGs were mainly associated with ion balance, transmembrane transport, and cell polarity by GO analysis, and the vesicle cycle, drug metabolism, and carcinogenesis processes by KEGG analysis (*Figure 6D,6E*).

MPP7 was significantly correlated with tumor-infiltrating immune cells in ccRCC

To better reveal the relationship between *MPP7* and immune status of ccRCC, we investigatde the potential association between *MPP7* expression and infiltration status of 24 immune cell types using R software. *MPP7* expression was significantly correlated with dendritic cells (DCs), $CD8^+$ T cells, cytotoxic cells, eosinophils, mast cells, T helper (Th) cells, macrophages, neutrophils, natural killer (NK) cells, central memory T cells (TCMs), Th1 cells, Th17 cells, and regulatory T cells (Tregs) (*Figure 7A,7B*). Using the TIMER tool, we further investigated the effects of *MPP7* and infiltrating cells on the survival rates of patients with ccRCC (*Figure 7C*). The results showed that naïve B cells, $CD4^+$ memory T cells, eosinophils, M1 macrophages, activated mast cells, neutrophils, activated NK cells, and T follicular helper cells (TFHs) were correlated with survival rates of ccRCC patients.

Further research showed that *MPP7* expression was positively correlated with the infiltration levels of eosinophils (r=0.150, P<0.001), mast cells (r=0.170, P<0.001), Th cells (r=0.142, P<0.001), and TCMs (r=0.186, P<0.001). In contrast, *MPP7* expression was negatively correlated with activated DCs (aDCs) (r=–0.219, P<0.001), CD8 T cells (r=–0.168, P<0.001), cytotoxic cells (r=–0.305, P<0.001), plasmacytoid DCs (pDCs) (r=–0.303, P<0.001), Th1 cells (r=–0.192, P<0.001), and Tregs (r=–0.313, P<0.001) (*Figure 7D*). These results indicated that *MPP7* participates in immune cell infiltration and immunity-associated clinical prognosis in ccRCC.

Discussion

Recent advances in understanding the molecular background of ccRCC have led to unprecedented progress in the therapeutic strategies of ccRCC (26). Also, developments have been made in molecularly targeted drugs in advanced ccRCC (27). However, ccRCC is a highly vascularized tumor and prone to distant metastasis. In this study, we mainly focused on *MPP7*, a critical polarity-related protein, which plays important roles in cell-cell

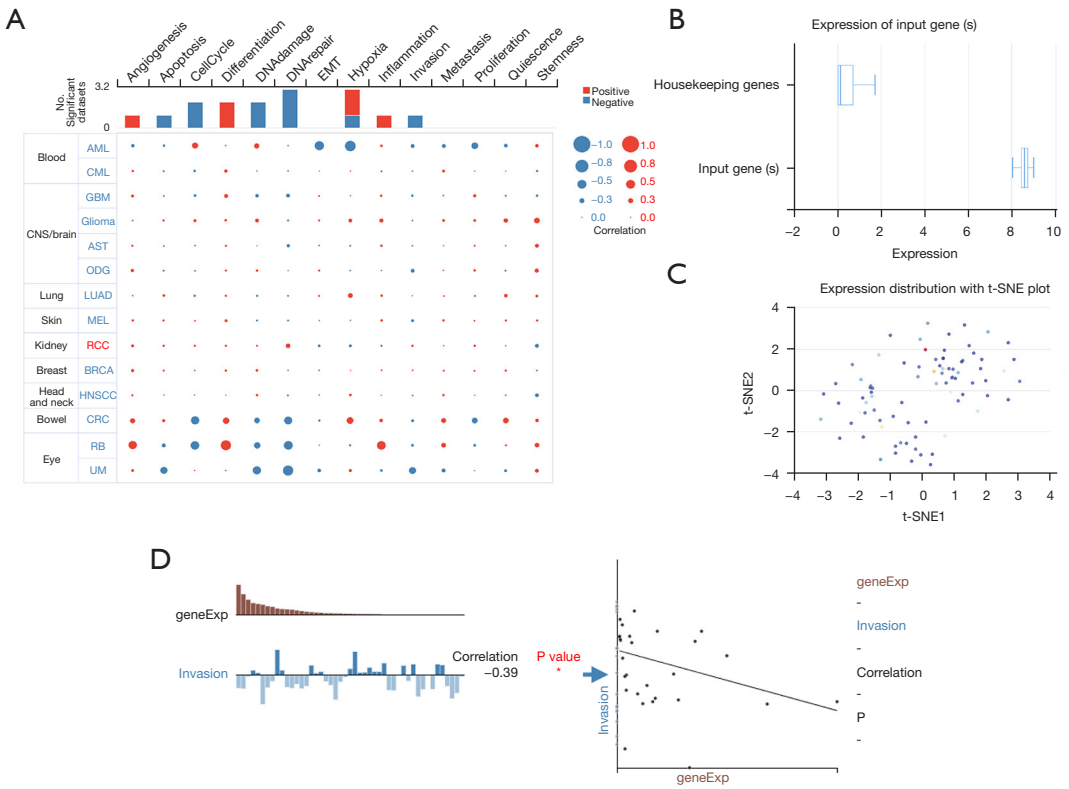

Figure 5 Single-cell sequencing analysis of *MPP7* in the functional states of ccRCC. (A) The CancerSEA database was used to reveal the associations between cancer hallmarks and *MPP7* expression. (B-D) A specific single-cell sequencing study concentrated on the role of *MPP7* in ccRCC. *P<0.05. EMT, epithelial-to-mesenchymal transition; CNS, central nervous system; t-SNE, t-distributed stochastic neighbor embedding; *MPP7*, membrane palmitoylated protein-7; ccRCC, clear cell renal cell carcinoma. AML, acute myelocytic leukemia; CML, chronic myelocytic leukemia; GBM, glioblastoma multiforme; AST, astrocytes; ODG, oligodendrogliomas; LUAD, lung adenocarcinoma; MEL, melanoma; BRCA, breast cancer; HNSCC, head and neck squamous cell carcinoma; CRC, colorectal cancer; RB, retinoblastoma; UM, uveal melanoma.

junction and adhesion. However, its role in ccRCC is still unknown. Using TCGA, GEO, and HPA databases, we confirmed that *MPP7* expression is decreased in ccRCC tissues compared to that in adjacent tissues. Dysregulated promoter methylation status contribute to the aberrant expression profile. *MPP7* expression was markedly correlated with key clinicopathological factors (M stage, pathological stage, histological grade, and survival status). Moreover, *MPP7* correlated with dysregulated immune filtration status of several cell types which was associated with clinical prognosis. Furthermore, KEGG and GO analyses revealed that *MPP7* functions in mitochondrial oxidative metabolism and ion balance. Therefore, *MPP7* could become a potential biomarker for prognostic prediction, combined with other key factors, while could function in the pathogenesis and progression of ccRCC in relation to mitochondrial or immune functions regulation.

A previous report has shown that changes in polarity-associated proteins affect epithelial polarity, thereby regulating cell proliferation, migration, and tumorigenesis (6). MPPs are a class of cell polarity-related proteins comprising a total of seven members (*MPP1* to *MPP7*), which play important roles in cell junctions and adhesion (8). Generally, the protein structure of MPP members contains a highly conserved core element composing of three sequentially-arranged domains. These three domains include a post-synaptic density protein 95/disc large/zonula occludens-1 (PDZ) domain, a Src homology 3 (SH3) domain and a catalytically inactive guanylate kinase (GUK) domain (8). This multidomain architecture and structure allow MPPs to form various protein-protein complexes, facilitating its function in signal transduction, secretion and maintaining cell polarity or

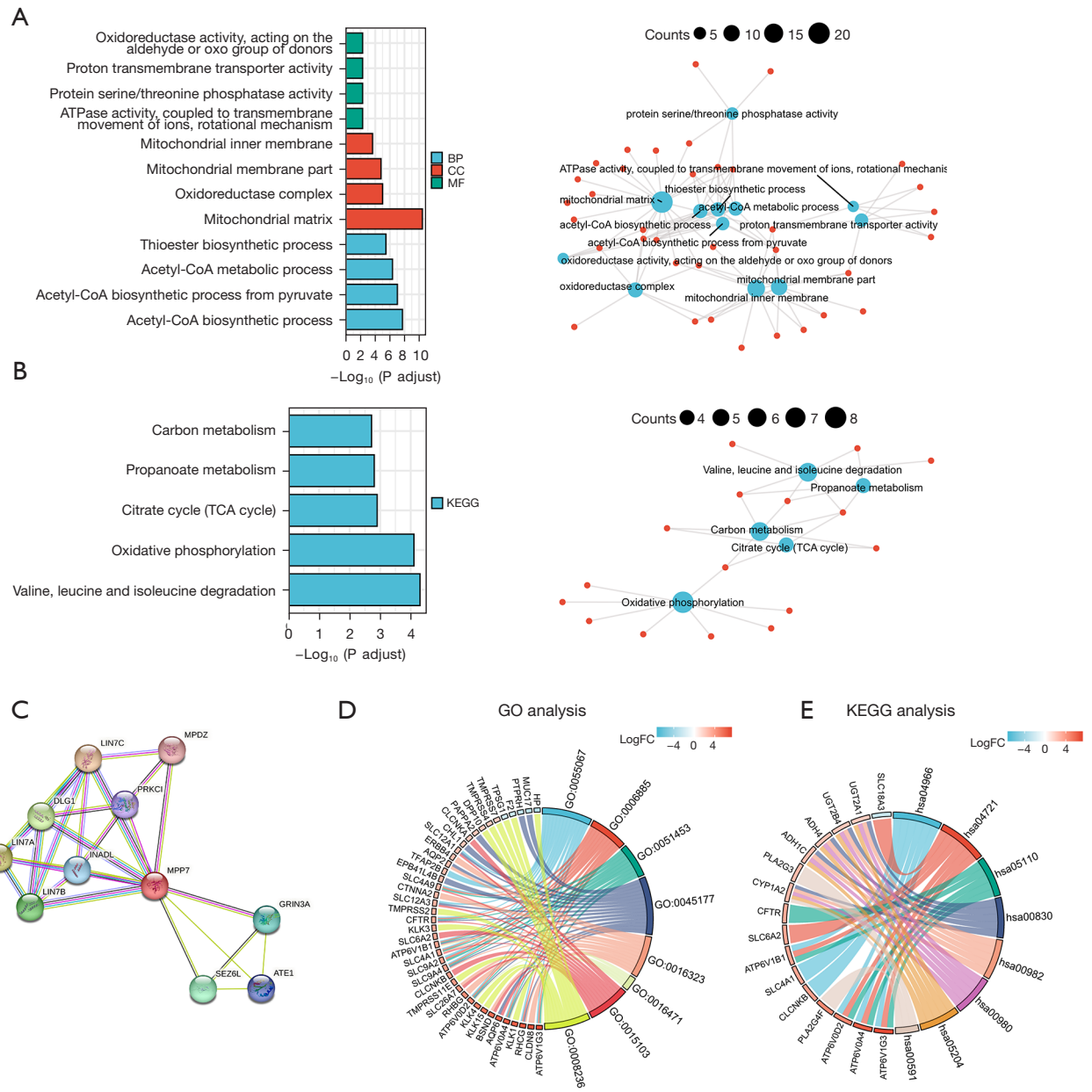

Figure 6 Functional and pathway enrichment analysis of *MPP7* in ccRCC. (A) Significant GO terms (including BP, MF, and CC) of the top 100 genes most associated with *MPP7*. (B) Significant KEGG pathway of the top 100 genes most associated with *MPP7*. (C) *MPP7*-binding proteins obtained using the STRING tool. (D,E) GO and KEGG analyses of DEGs associated with *MPP7* using TCGA-KIRC data. BP, biological process; CC, cell composition; MF, molecular function; KEGG, Kyoto Encyclopedia of Genes and Genome; TCA, tricarboxylic acid; GO, Gene Ontology; *MPP7*, membrane palmitoylated protein-7; ccRCC, clear cell renal cell carcinoma; DEGs, differentially expressed genes; TCGA, The Cancer Genome Atlas; KIRC, kidney renal clear cell carcinoma.

cell-cell adhesion (28-30). A previous study by Bohl *et al.* demonstrated that *MPP7* forms a tripartite complex with Discs large homolog 1 (*DLG1*) and Lin-7 homolog A (*LIN7A*) or Lin-7 homolog C (*LIN7C*), which regulates the stability and localization of *DLG1* to cell junctions (28). Therefore, it could be speculated that MPPs may participate in tumorigenesis and metastasis. Furthermore, it has also been shown that *MPP6* downregulation is associated with

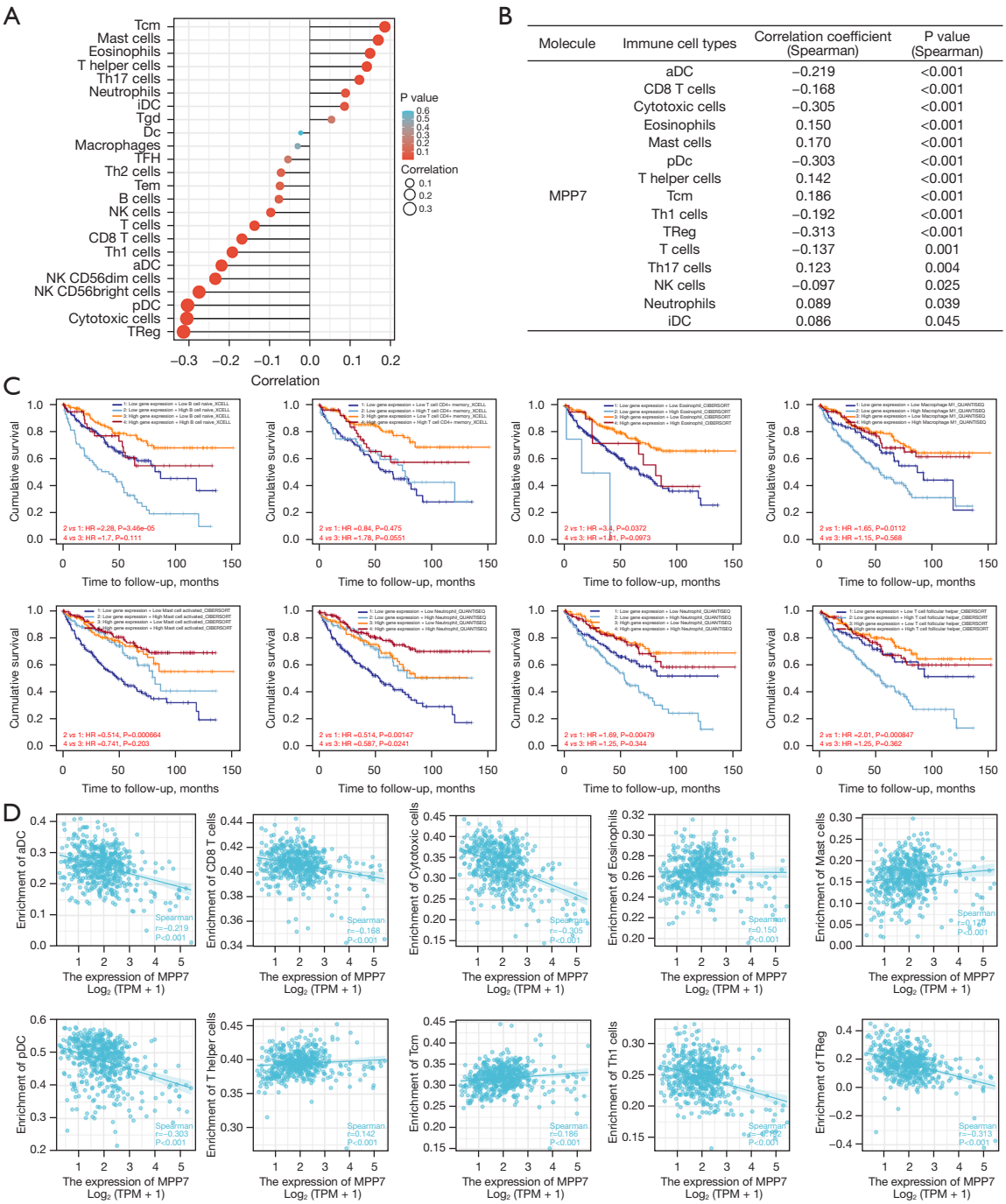

Molecule	Immune cell types	Correlation coefficient (Spearman)	P value (Spearman)
MPP7	aDC	−0.219	<0.001
	CD8 T cells	−0.168	<0.001
	Cytotoxic cells	−0.305	<0.001
	Eosinophils	0.150	<0.001
	Mast cells	0.170	<0.001
	pDc	−0.303	<0.001
	T helper cells	0.142	<0.001
	Tcm	0.186	<0.001
	Th1 cells	−0.192	<0.001
	TReg	−0.313	<0.001
	T cells	−0.137	0.001
	Th17 cells	0.123	0.004
	NK cells	−0.097	0.025
	Neutrophils	0.089	0.039
	iDC	0.086	0.045

Figure 7 Associations between *MPP7* expression and immune cell infiltration status of ccRCC. (A) Lollipop chart of the *MPP7* expression levels in 24 immune cells. (B) The immune cell infiltration status associated with *MPP7* expression with statistical significance. (C) The effects of immune cell infiltration on the prognoses in ccRCC patients. (D) Correlation between *MPP7* expression and immune cell infiltration levels, including the aDCs, CD8 T cells, cytotoxic cells, eosinophils, mast cells, pDCs, Th cells, TCMs, Th1 cells, Tregs. TCMs, central memory T cells; Th, T helper; iDCs, immature DCs; DCs, dendritic cells; Tgd, T gamma delta; TFHs, T follicular helper cells; NK, natural killer; aDCs, activated DCs; pDCs, plasmacytoid DCs; Tregs, regulatory T cells; HR, hazard ratio; *MPP7*, membrane palmitoylated protein-7; TPM, transcripts per million; ccRCC, clear cell renal cell carcinoma; *MPP7*, membrane palmitoylated protein-7.

ovarian cancer progression (10). The inhibition of *MPP6* can reverse the antitumor activity of Saa3-null cancer-associated fibroblasts (11). Moreover, *MPP7* functions in both pancreatic ductal adenocarcinoma and breast cancer by modulating autophagy and activating the EGFR/AKT signaling, respectively (12,13). In this study, we systematically analyzed the role of *MPP7* in the clinical outcomes of ccRCC; our results showed that *MPP7* was correlated with metastasis stage, pathological stage, histological grade, and survival status. More importantly, *MPP7* functions in immune infiltration, which may be attributed to the complex protein interactions between the tumor and immune cells. Therefore, *MPP7* could be a useful biomarker and a potential therapeutic target for ccRCC patients. However, the effects of *MPP7* on tumor proliferation, invasion and metastasis should be validated using both cellular and animal experiments with strict controls.

The tumor microenvironment (TME) comprises both tumor cells and various types of immune cells, and functions in tumor progression, metastasis, and treatment resistance (31). Given that *MPP7* is a critical gene in cell junctions and adhesion, we speculated that *MPP7* affects the TME by modulating the interactions and infiltration of immune cells and tumor cells. In the present study, we systematically analyzed the correlations between *MPP7* and immune cell infiltration as well as the associated clinical prognosis. Our findings showed that *MPP7* expression was positively correlated with the infiltration levels of eosinophils, mast cells, Th cells, and TCMs, but was negatively correlated with aDCs, CD8 T cells, cytotoxic cells, pDCs, Th1 cells, and Tregs. Also, the TME comprises a variety of immune cell types that influence tumor cell survival and clinical prognosis. Therefore, we can speculate that *MPP7* functions in TME by affecting the immune status of TME. Future studies are needed to further explore the relationship between *MPP7* and the functional regulation of these cell types.

To determine the pathways in which *MPP7* is involved, a functional analysis of both co-expressed genes and DEGs was conducted using GO/KEGG. Interestingly, we found that most of the *MPP7*-related genes were associated with the mitochondrial membrane, citrate cycle, and oxidative phosphorylation, instead of cell junction proteins, indicating that *MPP7* functions in mitochondrial metabolism and redox regulation. However, previous studies did not report on the relationship between MPPs and mitochondrial functions. Therefore, in addition to its role in cell adhesion, *MPP7* might become an important target in mitochondrial metabolism. However, the relationship between *MPP7* and mitochondrial functions is still not clear and further studies are needed to explore the role of *MPP7* on redox status, energy metabolism, mitochondrial dynamics and cell death.

Energy and mitochondrial metabolism have been shown to play important roles in cancer pathogenesis and progression. Metabolic demands alterations frequently occur during tumor initiation, progression, and metastasis, challenging our understanding of tumor biology and resulting in the development of novel therapeutics. In particular, RCC is considered to be more prone to metabolic disease, with unique glucose and lipid metabolism patterns (32). Wu *et al.* reported that redox-related genes could accurately predict ccRCC prognosis (33). Xing *et al.* revealed that glycolysis-related genes could predict OS in ccRCC (34). Meanwhile, tumor-associated immune cells function in the carcinogenesis and treatment of ccRCC (35). Therefore, *MPP7* may become an important connection between energy metabolism and immune status in both cancer pathogenesis and treatment.

Although our study has systematically explored the relationship between *MPP7* expression and ccRCC in bioinformatic manner, it has some limitations that should be noted. Firstly, most of the data analyzed by bioinformatics methods were downloaded directly from public databases, and our findings require systematical experimental investigations. Secondly, a longer follow-up is required to validate *MPP7* as an accurate prognostic predictor for ccRCC patients.

Conclusions

In this study, we report the role of MPP7 in the prognostic prediction of ccRCC for the first time, combining with other key factors. MPP7 was associated with mitochondrial metabolism, immune infiltration, and ion balance, which may be an important link between energy metabolism and immunity of cancer. Therefore, MPP7 could be a potential prognostic biomarker and therapeutic target for ccRCC, combined with other key factors. Further mechanistic studies are needed to validate our findings.

Acknowledgments

We acknowledge TCGA, GEO, and HPA databases for providing their platforms and contributors for uploading their meaningful datasets. The results published here are in

part based on data generated by TCGA Research Network: https://www.cancer.gov/tcga.
Funding: This study was funded by the Specialized Scientific Research Project of Military Health Care (No. 21BJZ37), the Hainan Provincial Natural Science Foundation of China (No. 821QN383), and the National Natural Science Foundation of China (No. 82270769).

Footnote

Reporting Checklist: The authors have completed the REMARK reporting checklist. Available at https://tau.amegroups.com/article/view/10.21037/tau-23-166/rc

Peer Review File: Available at https://tau.amegroups.com/article/view/10.21037/tau-23-166/prf

Conflicts of Interest: All authors have completed the ICMJE uniform disclosure form (available at https://tau.amegroups.com/article/view/10.21037/tau-23-166/coif). The authors have no conflicts of interest to declare.

Ethical Statement: The authors are accountable for all aspects of the work in ensuring that questions related to the accuracy or integrity of any part of the work are appropriately investigated and resolved. The study was conducted in accordance with the Declaration of Helsinki (as revised in 2013).

References

1. Miller KD, Nogueira L, Devasia T, et al. Cancer treatment and survivorship statistics, 2022. CA Cancer J Clin 2022;72:409-36.
2. Grimaldo-Roque HJ, Martinez-Castaneda EA, Morales-Garcia MG, et al. Impact of the Discordance Between Scales of Memorial Sloan-Kettering Cancer Center and International Metastatic Renal Cell Carcinoma Database Consortium in Patients' Prognosis With Metastatic Renal Cancer. World J Oncol 2022;13:53-8.
3. Ljungberg B, Albiges L, Abu-Ghanem Y, et al. European Association of Urology Guidelines on Renal Cell Carcinoma: The 2022 Update. Eur Urol 2022;82:399-410.
4. Larroquette M, Lefort F, Heraudet L, et al. Therapeutic Management of Metastatic Clear Cell Renal Cell Carcinoma: A Revolution in Every Decade. Cancers (Basel) 2022;14:6230.
5. Choueiri TK, Halabi S, Sanford BL, et al. Cabozantinib Versus Sunitinib As Initial Targeted Therapy for Patients With Metastatic Renal Cell Carcinoma of Poor or Intermediate Risk: The Alliance A031203 CABOSUN Trial. J Clin Oncol 2017;35:591-7.
6. Gandalovičová A, Vomastek T, Rosel D, et al. Cell polarity signaling in the plasticity of cancer cell invasiveness. Oncotarget 2016;7:25022-49.
7. Ye F, Zeng M, Zhang M. Mechanisms of MAGUK-mediated cellular junctional complex organization. Curr Opin Struct Biol 2018;48:6-15.
8. Chytła A, Gajdzik-Nowak W, Olszewska P, et al. Not Just Another Scaffolding Protein Family: The Multifaceted MPPs. Molecules 2020;25:4954.
9. Baumgartner M, Weiss A, Fritzius T, et al. The PDZ protein MPP2 interacts with c-Src in epithelial cells. Exp Cell Res 2009;315:2888-98.
10. Xu F, Si X, Du J, et al. Downregulating SynCAM and MPP6 expression is associated with ovarian cancer progression. Oncol Lett 2019;18:2477-83.
11. Djurec M, Graña O, Lee A, et al. Saa3 is a key mediator of the protumorigenic properties of cancer-associated fibroblasts in pancreatic tumors. Proc Natl Acad Sci U S A 2018;115:E1147-56.
12. Liao W, Fan L, Li M, et al. MPP7 promotes the migration and invasion of breast cancer cells via EGFR/AKT signaling. Cell Biol Int 2021;45:948-56.
13. New M, Van Acker T, Sakamaki JI, et al. MDH1 and MPP7 Regulate Autophagy in Pancreatic Ductal Adenocarcinoma. Cancer Res 2019;79:1884-98.
14. Cheng Y, Xu T, Li S, et al. GPX1, a biomarker for the diagnosis and prognosis of kidney cancer, promotes the progression of kidney cancer. Aging (Albany NY) 2019;11:12165-76.
15. Ruan H, Bao L, Song Z, et al. High expression of TAZ serves as a novel prognostic biomarker and drives cancer progression in renal cancer. Exp Cell Res 2019;376:181-91.
16. Song Q, Zheng Y, Wu J, et al. PTP4A3 Is a Prognostic Biomarker Correlated With Immune Infiltrates in Papillary

Renal Cell Carcinoma. Front Immunol 2021;12:717688.
17. Wang Q, Li Z, Zhou S, et al. NCAPG2 could be an immunological and prognostic biomarker: From pan-cancer analysis to pancreatic cancer validation. Front Immunol 2023;14:1097403.
18. Colwill K; Renewable Protein Binder Working Group; Gräslund S. A roadmap to generate renewable protein binders to the human proteome. Nat Methods 2011;8:551-8.
19. Modhukur V, Iljasenko T, Metsalu T, et al. MethSurv: a web tool to perform multivariable survival analysis using DNA methylation data. Epigenomics 2018;10:277-88.
20. Shang BB, Chen J, Wang ZG, et al. Significant correlation between HSPA4 and prognosis and immune regulation in hepatocellular carcinoma. PeerJ 2021;9:e12315.
21. Zhou Q, Hou Z, Zuo S, et al. LUCAT1 promotes colorectal cancer tumorigenesis by targeting the ribosomal protein L40-MDM2-p53 pathway through binding with UBA52. Cancer Sci 2019;110:1194-207.
22. Szklarczyk D, Gable AL, Lyon D, et al. STRING v11: protein-protein association networks with increased coverage, supporting functional discovery in genome-wide experimental datasets. Nucleic Acids Res 2019;47:D607-13.
23. Li T, Fan J, Wang B, et al. TIMER: A Web Server for Comprehensive Analysis of Tumor-Infiltrating Immune Cells. Cancer Res 2017;77:e108-10.
24. Newman AM, Liu CL, Green MR, et al. Robust enumeration of cell subsets from tissue expression profiles. Nat Methods 2015;12:453-7.
25. Kim KT, Lee HW, Lee HO, et al. Application of single-cell RNA sequencing in optimizing a combinatorial therapeutic strategy in metastatic renal cell carcinoma. Genome Biol 2016;17:80.
26. Miao D, Margolis CA, Gao W, et al. Genomic correlates of response to immune checkpoint therapies in clear cell renal cell carcinoma. Science 2018;359:801-6.
27. Srivastava A, Doppalapudi SK, Patel HV, et al. The roaring 2020s: a new decade of systemic therapy for renal cell carcinoma. Curr Opin Oncol 2022;34:234-42.
28. Bohl J, Brimer N, Lyons C, et al. The stardust family protein MPP7 forms a tripartite complex with LIN7 and DLG1 that regulates the stability and localization of DLG1 to cell junctions. J Biol Chem 2007;282:9392-400.
29. Stucke VM, Timmerman E, Vandekerckhove J, et al. The MAGUK protein MPP7 binds to the polarity protein hDlg1 and facilitates epithelial tight junction formation. Mol Biol Cell 2007;18:1744-55.
30. Podkalicka J, Biernatowska A, Majkowski M, et al. MPP1 as a Factor Regulating Phase Separation in Giant Plasma Membrane-Derived Vesicles. Biophys J 2015;108:2201-11.
31. Kim MC, Jin Z, Kolb R, et al. Updates on Immunotherapy and Immune Landscape in Renal Clear Cell Carcinoma. Cancers (Basel) 2021;13:5856.
32. Qi X, Li Q, Che X, et al. The Uniqueness of Clear Cell Renal Cell Carcinoma: Summary of the Process and Abnormality of Glucose Metabolism and Lipid Metabolism in ccRCC. Front Oncol 2021;11:727778.
33. Wu Y, Wei X, Feng H, et al. Integrated Analysis to Identify a Redox-Related Prognostic Signature for Clear Cell Renal Cell Carcinoma. Oxid Med Cell Longev 2021;2021:6648093.
34. Xing Q, Zeng T, Liu S, et al. A novel 10 glycolysis-related genes signature could predict overall survival for clear cell renal cell carcinoma. BMC Cancer 2021;21:381.
35. Zarrabi K, Walzer E, Zibelman M. Immune Checkpoint Inhibition in Advanced Non-Clear Cell Renal Cell Carcinoma: Leveraging Success from Clear Cell Histology into New Opportunities. Cancers (Basel) 2021;13:3652.

(English Language Editor: A. Kassem)

Cite this article as: Cheng X, Sun D, Li H, Zhang J, Luo Q, Jin X, Chen Y, Yuan Q, Wang B. *MPP7* is a potential prognostic marker and is associated with cancer metabolism and immune infiltration in clear cell renal cell carcinoma: a bioinformatics analysis based on the TCGA database. Transl Androl Urol 2023;12(4):642-658. doi: 10.21037/tau-23-166

